NANO · MICRO small
www.small-journal.com

Nanoliter Scale Parallel Liquid–Liquid Extraction for High-Throughput Purification on a Droplet Microarray

*Janne J. Wiedmann, Yelda N. Demirdögen, Stefan Schmidt, Mariia A. Kuzina, Yanchen Wu, Fei Wang, Britta Nestler, Carsten Hopf, and Pavel A. Levkin**

In the current drug discovery process, the synthesis of compound libraries is separated from biological screenings both conceptually and technologically. One of the reasons is that parallel on-chip high-throughput purification of synthesized compounds is still a major challenge. Here, on-chip miniaturized high-throughput liquid–liquid extraction in volumes down to 150 nL with efficiency comparable to or better than large-scale extraction utilizing separation funnels is demonstrated. The method is based on automated and programmable merging of arrays of aqueous nanoliter droplets with organic droplets. Multi-step extraction performed simultaneously or with changing conditions as well as handling of femtomoles of compounds are demonstrated. In addition, the extraction efficiency is analyzed with a fast optical readout as well as matrix-assisted laser desorption ionization-mass spectrometry on-chip detection. The new massively parallel and miniaturized purification method adds another important tool to the chemBIOS concept combining chemical combinatorial synthesis with biological screenings on the same miniaturized droplet microarray platform, which will be essential to accelerate drug discovery.

1. Introduction

Discovering new drugs is one of the major tasks to enable health and wellbeing for the whole population on Earth. Nevertheless, drug development bears high risks and extremely high costs.[1] The whole process usually takes more than 10 years and up to 2.6 billion USD, while only one out of 10 000 compounds is finally approved as a new drug.[2] Only around 50 drugs are approved by the FDA in a year and there is a high demand to continue and improve this trend. Especially thinking about orphan drugs, it is important to reduce the time and cost consumption in all stages of the drug development process.[1] In order to accelerate development of novel functional materials, chemicals, or drug candidates, high-throughput and miniaturized synthetic methods are important.[3] Integration of such miniaturized synthesis with biological high-throughput screenings (chemBIOS approach)[4–6] is essential to get rid of the technological and conceptual gap between these two steps in drug discovery.[7] This is necessary to accelerate the hit detection and optimization in the early stage of drug development, which can usually take 6 years or more.[8] Until now, this has been challenging partly due to the necessity of purification of synthesized compounds in highly miniaturized and in parallel high-throughput way.[9] Moreover, the purification methods have to be compatible with the same platform to be used for both synthesis and biological screenings. For this reason, the overwhelming majority of miniaturized high-throughput synthesis methods is still done using solid-phase synthesis (SPS), thus, allowing simple removal of side products and added reagents by washing.[10]

J. J. Wiedmann, Y. N. Demirdögen, M. A. Kuzina, P. A. Levkin
Institute of Biological and Chemical Systems – Functional Molecular Systems (IBCS-FMS), Karlsruhe Institute of Technology (KIT)
Hermann-von-Helmholtz-Platz 1
76344 Eggenstein-Leopoldshafen, Germany
E-mail: levkin@kit.edu

The ORCID identification number(s) for the author(s) of this article can be found under https://doi.org/10.1002/smll.202204512.

DOI: 10.1002/smll.202204512

S. Schmidt, C. Hopf
Center for Mass Spectrometry and Optical Spectroscopy (CeMOS)
Mannheim University of Applied Sciences
Paul-Wittsack-Straße 10, 68163 Mannheim, Germany

Y. Wu, F. Wang, B. Nestler
Institute for Applied Materials – Microstructure Modelling and Simulation
Karlsruhe Institute of Technology (KIT)
Strasse am Forum 7, 76131 Karlsruhe, Germany

C. Hopf
Medical Faculty
Mannheim Center for Translational Neuroscience (MCTN)
Heidelberg University
Theodor Kutzer-Ufer 1–3, 68167 Mannheim, Germany

P. A. Levkin
Institute of Organic Chemistry (IOC)
Karlsruhe Institute of Technology (KIT)
Kaiserstraße 12, 76131 Karlsruhe, Germany

For SPS, large one bead one compound libraries are synthesized using beads as solid supports with a split and mix reaction path in either syringes[11] or miniaturized in microtiter plates.[12] To achieve spatial resolution on an array format, SPOT synthesis was developed by Frank 30 years ago.[13] There, the starting material is bound to a cellulose membrane, followed by addition of single droplets containing reagents. The droplet size and position defines the area and format of the array.[14] Another possibility for dense, spatially defined arrays is the photolithographic approach from Fodor et al., where photolabile protection groups are used in combination with photolithography.[15] Brehm et al. developed the SPS on the droplet microarray platform using a polymer film decorated with an array of spots with reactive groups separated by a pattern of hydrophobic groups.[16] This patterned surface allows higher stability and miniaturization compared to the SPOT method.[6] Solid phase synthesis, however, usually needs excess of reagents and solvents, making it less sustainable. Furthermore, the covalent binding to a solid support limits the choice of reactions, starting materials, and amount of synthesized compounds, and additionally requires a cleavage step.[17]

High-throughput synthetic methods use high-performance liquid chromatography (HPLC) for 384-well plates,[18] precipitation in 96-well format[19] or two or three phase microfluidic chips[20] for purification. In most of the cases, crude reaction mixtures containing side products were used for screening the activity by biochemical binding assays, which are less sensitive to impurities than cellular assays.[21][4]

Liquid–liquid extraction (LLE) is one of the most powerful and traditional purification method, which is used in most of organic syntheses performed both in the labs and at industrial scale.[22] There are few approaches reported for miniaturization of the process: for example, extractions were performed with automated liquid handling systems to add and remove the organic phase in microliter plates.[23] Sun et al. used capillaries combined with microfluidic robotics or extractions from 800 nL droplets into 10 nL droplets covered by a layer of oil to prevent evaporation.[24] For slug-flow microfluidic extraction, multiple extractions were carried out in a capillary, while the droplets were separated by an immiscible carrier fluid.[25] For Single Drop Microextraction (SDME), a microsyringe is used to immerse the extraction phase directly in the sample or to place it above.[30] All reported methods required complex instrumental settings to enable the handling of both phases during merging, extraction, and separation, especially if a large library has to be purified in one step.

Recently, the Droplet Microarray (DMA) platform was developed.[26] The DMA, consisting of a microscopic glass slide patterned with hydrophilic spots, separated by omniphobic, or superhydrophobic borders, enables both chemical reactions[16] and biological experiments in 100 nL droplet arrays[27] and is compatible with various on-chip analytical methods.[5,28] In this work, we utilized an omniphobic–omniphilic pattern based on a dendrimeric surface functionalization according to Benz et al.[4,5,16]

Thus, the DMA platform can be used for the chemBIOS concept integrating both chemistry and biology.[29] Nevertheless, the purification of organic compounds on DMA has proved to be challenging. Till now, solid-phase synthesis at nanomolar scale was shown by Brehm et al. using the DMA for combinatorial peptide synthesis[6] and the Ugi 4-component reaction.[6] Excess of reagents and side products were removed by rinsing the whole slide before cleaving the product from the polymer support. LLE was also demonstrated by sandwiching two patterned slides, where each slide contained one of the liquid phases. In this case, the manual handling did not allow any miniaturization below 3 μL, however.[5]

Here, we demonstrate a new method for miniaturized, high-throughput liquid–liquid extractions performed directly on the DMA using 75–300 nL droplets (**Figure 1**). Organic and aqueous phases are combined by dispensing two droplets onto a patterned substrate close to each other, so that they form a liquid–liquid interphase of around 0.25 mm^2. We demonstrate efficient extraction without shaking and independent of the solvent density. After extraction, the droplets are automatically separated due to the combination of evaporation and dewetting from the omniphobic borders. The efficiency of the extraction is shown using both microscopy and Matrix-assisted laser desorption ionization-mass spectrometry (MALDI-MS). Possibilities to increase efficiency by multiple extractions from different sites and selective separation of mixtures as well as efficient extraction in the femtomole range was demonstrated.

2. Results and Discussion

Miniaturized LLE experiments were performed on the recently developed DMA. The DMA slides were prepared based on the method developed by Benz et al.[5] For increased density of functional groups and improved omniphobic/omniphilic character, a microscopic glass slide was functionalized with dendrimeric structures by repeating an esterification and UV-mediated thiol-ene reaction steps. In the last step, thioglycerol and 1H,1H,2H,2H-perfluorodecanethiol were used in the thiol-ene reaction to create omniphilic spots (900 μm × 900 μm) and omniphobic borders (225 μm wide), respectively. The square spots separated by the repelling border could accommodate between 100 and 300 nL droplets of either aqueous or organic solvents such as *N,N*-dimethylformamide and 1-octanol. A patterned glass slide with a dimension of 75.6 × 25.0 × 1.00 mm contains 1152 (18 × 64) omniphilic spots. Side views of water and 1-octanol droplets added with a non-contact liquid dispenser (Figure S1, Supporting Information) and contact angles can be found in Figure S2, Supporting Information.

The concept of the miniaturized extraction demonstrated within this work is shown in **Figure 2**A. First, aqueous droplets, containing a compound to be extracted are dispensed to form droplets of 200 nL. Organic solvent is added directly on the border between the aqueous donor droplet and the neighboring omniphilic spot (Figure 2A-i) to bring the two droplets in contact, thereby creating the organic-water interface (Figure 2A-ii). For a whole DMA slide with 192 spots, the two dispensing steps are finished within 2 min. The interfacial area of two contact immiscible droplets in equilibrium as a function of the droplet volume was calculated by the so-called phase-field model.[30] In this model, we used the static contact angles of the droplets on omniphilic and omniphobic surfaces as well as the equilibrium contact angle at the triple junction of

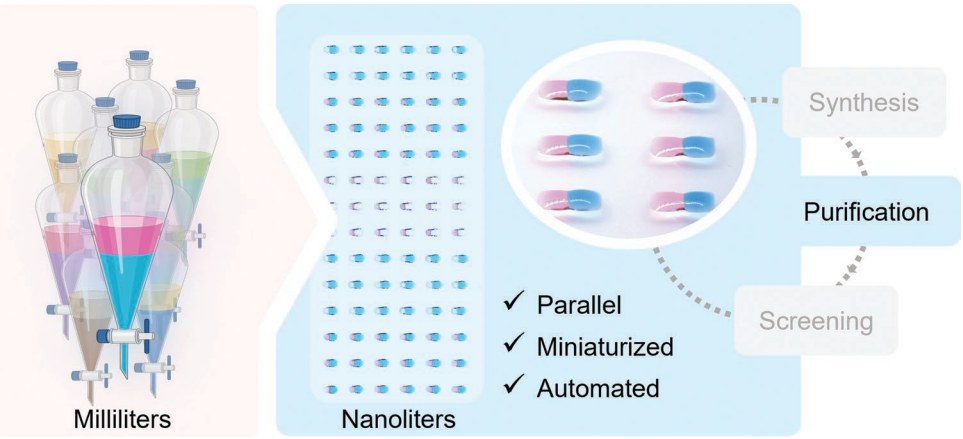

Figure 1. Concept of on-chip high-throughput parallel purification of compounds via LLE. LLE in the lab is usually performed using separation funnels (left). In this work, LLE is miniaturized and parallelized using DMAs enabling individual extractions from 200 nL droplets (right), which is an essential part of the process of combinatorial on-chip synthesis of compound libraries and its integration with biological assays.

organic-aqueous-surrounding. The model shows that the contact area of the two immiscible droplets can be depicted by a segment with chord length s and sagitta length h (Figure S3, Supporting Information). For two droplets with the same volume of 200 nL, the contact area from the phase-field model calculation is 0.25 mm^2. Due to the omniphilic surface of the neighboring spot, the organic droplet fills the neighboring empty spot. The extraction between the two phases starts as soon as the interface is formed (Figure 2A-iii,iv).

The extraction at this scale takes 60 s to extract 40 pmol of Rhodamine B from an aqueous 200 nL droplet into a 100 nL droplet of 1-octanol (Figure 2B). Using the same concentration of 0.2 mM Rhodamine B in water in a bulk experiment with 100 mL of each solvent, 20 µmol must be extracted, which is 0.5×10^6 higher than in the droplet. For a separation funnel with a diameter of 7 cm at the interphase, the area for material exchange is only increasing by 0.5×10^4 compared to the droplet. This lower decrease in the surface area compared to the decreasing amount of extracted compound shows a big advantage of the miniaturized droplet format of the DMA. Due to the optimized ratio of compound to interfacial area, the extraction does not require any shaking of the system as it is done in bulk.

The separation of the organic and aqueous droplets takes place spontaneously upon evaporation of the droplet with lower vapor pressure (Figure 2A-v). Evaporation of one of the droplets leads to the reduction of the liquid–liquid interface, which triggers spontaneous separation of the two droplets: aqueous droplet stays in the omniphilic spot, while the organic droplet is retracted from the omniphobic border to the neighboring omniphilic spot (Figure 2A-vi).

The extraction of Rhodamine B (Figure 2C) from water to 1-octanol and droplet splitting is shown in Figure 2B. The Log P value of Rhodamine B is 1.95 and describes the distribution of the compound between an aqueous and 1-octanol phase.[31] With the value being positive, it is expected to accumulate in the organic phase. 1-Octanol has a vapor pressure of 8.7 Pa at 20 °C[32] and can form stable droplets on an omniphilic spot with up to 100 nL for 10 min without significant evaporation (Figure S2, Supporting Information). A 300 nL water droplet evaporated after 4 min due to the much higher vapor pressure of 3.17 kPa[33] (Figure S2, Supporting Information), which makes the evaporation of the aqueous phase the separation inducing step in this solvent system. Figure 2F demonstrates the possibility of parallel high-throughput miniaturized extraction of Rhodamine B (0.2 mM) from 192 × 200 nL aqueous droplets into 192 × 75 nL 1-octanol droplets. The dispensing of both phases was completed in 2 min and required 38.4 µL aqueous droplets and 14.4 µL of 1-octanol in total. The slide was imaged by a microscope or document scanner (Figure S1, Supporting Information), which resulted in a very fast analysis of multiple parallel extractions.

Quantification of the extracted droplets using images produced by a color scanner and calibration curve (Figure S3, Supporting Information) shows final concentration of Rhodamine B in 1-octanol droplets of 0.402 +/− 0.02 nM, which equals an extraction efficiency of 60 +/− 3%. The values were calculated out of 25 randomly picked spots from all regions of the slide and the low standard deviation shows the homogeneity. Furthermore, the droplet separation happens spontaneously triggered by evaporation, whereas bulk traditional extraction requires manual separation of the two phases. The separation of all 192 droplets took 10 min if the slide was placed in a fume hood. This time could be controlled. Thus, by placing the slide in a desiccator containing a liquid absorber under reduced pressure, the separation time was reduced to 3 min, while incubation of the slide in a closed petri dish with 100% humidity increased the merging of the droplets for 15 min. The corresponding extraction efficiency after 3 and 25 min extraction time was 55 +/− 2% and 65 +/−2%, respectively.

Next, we compared the miniaturized extraction performed on the DMA using 100 nL of 1-octanol to a laboratory scale 10 mL using a separation funnel in terms of extraction efficiency and time. To 10 mL Rhodamine B water solution (0.2 mM) different volumes of 1-octanol were added, followed by either static extraction for 10 min or extraction under agitation conditions for 1 min. Samples of the aqueous phase were taken and analyzed measuring the absorption at 554 nm to quantify the concentration of Rhodamine B left in the aqueous phase based on a calibration curve (Figure S4, Supporting Information). The results in Figure 2D demonstrate that the

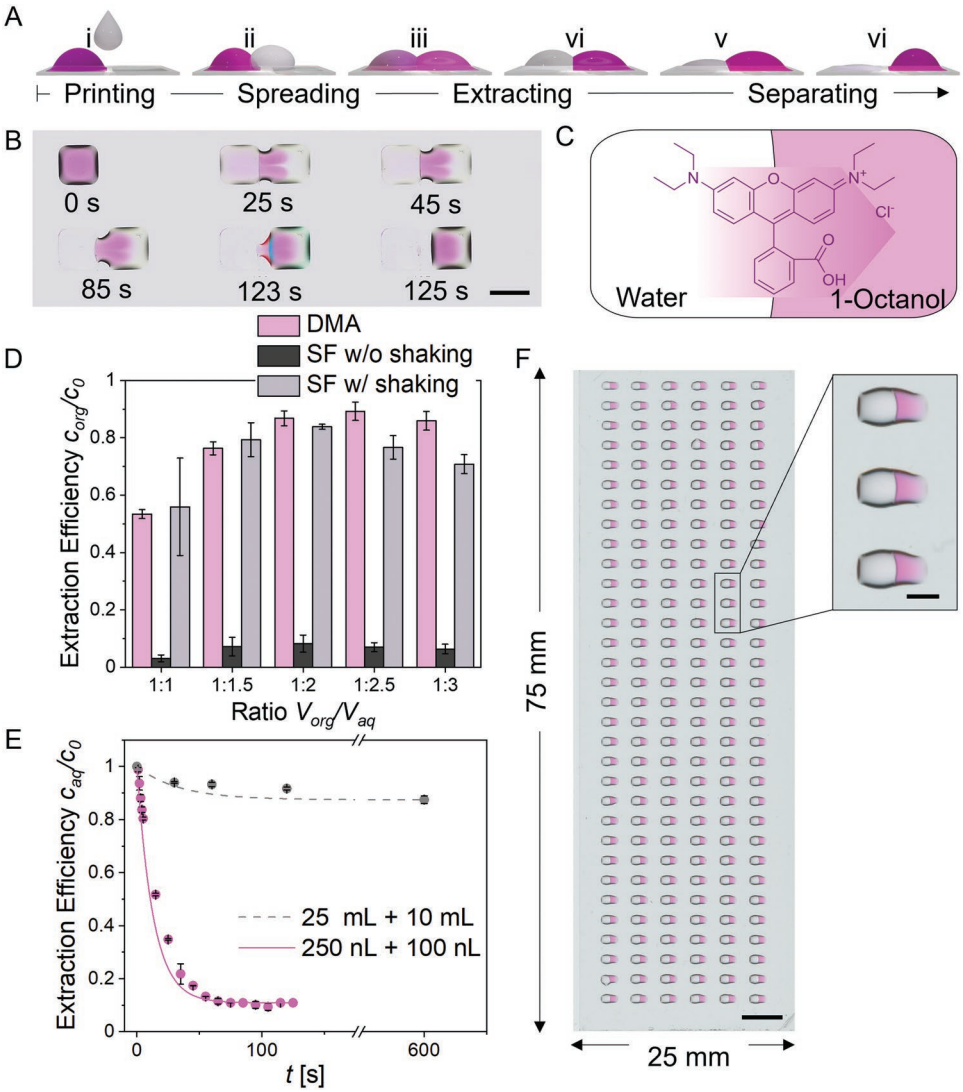

Figure 2. Description of the high-throughput, miniaturized parallel liquid–liquid extraction. A) Experimental setup of the on-chip extraction: the organic solvent is printed on the omniphobic border between the omniphilic spots (i) and an interface between the droplets is created (ii–iv). The droplet is spreading to the next omniphilic spot. After extraction, the droplets are separated by evaporation of the aqueous phase (v–vi). B) Extraction process of one 200 nL water droplet containing 0.2 M Rhodamine B to the neighbored droplet on the right containing 100 nL 1-octanol in 125 s. Scale bar is 1 mm. C) Schematic description of the extraction procedure of Rhodamine B from water (left) to 1-octanol (right). D) Extraction efficiency on the DMA (pink) compared to a conventional separation funnel (SF) with (w/, grey) and without (w/o, black) agitation. The efficiency is calculated by the ratio of the concentration before (c_0) and after extraction I. E) Time resolved extraction of Rhodamine B without agitation in milliliter (grey) and nanoliter (pink) scale. The concentration in the aqueous phase is given compared to the initial concentration. The non-linear fits show the trends. F) Top view of 192 parallel extractions of 0.2 mM Rhodamine B solution from water (left spot) to 1-octanol (right spot), scale bar is 5 mm. Scale bar for the magnified region is 2 mm.

best extraction efficiency was found for a volume ratio of 1:2.5 aqueous/organic phase for DMA and 1:2 for the separation funnel. The static extraction at 10 mL scale resulted only in 8 +/− 3% efficiency, while the 100 nL on-chip extraction showed from 53 +/− 1% to 89 +/− 3% efficiencies depending on the volume ratios. The efficiency was calculated out of ten randomly picked spots for each ratio. The bulk extraction under agitation was comparable to the static on-chip miniaturized extraction. With a single extraction in the same ratio of aqueous to organic solvent, both methods showed moderate efficiencies with 53% for the DMA and 56% for the separation funnel. By increasing the volume of the aqueous phase, the best extraction efficiency for the DMA was found for 250 nL at a ratio of 1:2.5 with 89% extraction, whereas the separation funnel showed lower performance at this ratio with only 77% efficiency. These results indicate that miniaturization of the extraction to nanoliter scale significantly improves the efficiency and even static extraction is enough to reach higher performance than bulk extraction at milliliter scale, thereby showing the feasibility of high-throughput miniaturized extraction.

In Figure 2E, the time scale for the static extraction of 10 mL is compared to the miniaturized extraction of 100 nL. The concentration of Rhodamine B in the aqueous phase was determined at different time points ranging from 1 s to 10 min. The

bulk sample was extracted without agitation and the extraction efficiency reached the limit after 10 min with still 87 +/− 1% of the dye remaining in the aqueous phase. For the miniaturized extraction, the process was stopped by the evaporation of the aqueous phase after 2 min with 11 +/− 1% remaining Rhodamine B on the spot of the aqueous droplet. This graph highlights the fast extraction process while maintaining a high extraction efficiency.

In order to further increase the extraction efficiency, we adapted the approach of multiple extractions from the bulk extraction in a separation funnel. One to four droplets of 100 nL 1-octanol were dispensed surrounding the centered spot containing 300 nL of 0.2 mM Rhodamine B aqueous solution (**Figure 3**A) in directly following dispensing steps. In contrast to extractions in the separation funnel, the extraction was still carried out at one time interval, but the efficiency increased with the number of 1-octanol droplets connected to the centered aqueous spot. The resulting extraction efficiency in Figure 3B was calculated by determining the color intensity in all 1-octanol droplets separately. With the calibration curve (Figure S4, Supporting Information), the amount of Rhodamine B extracted to each spot and, hence, the extraction efficiency was calculated. Summed up, this led to the total extraction efficiency of Rhodamine B. Starting at 86 +/− 3% for one single extraction, the efficiency was first reduced slightly, but was then increased to yield 95 +/− 6% if all four neighbored spots contained 1-octanol. Comparing the color intensity of all 1-octanol droplets around an aqueous spot, a concentration gradient of Rhodamine B is visible. This can be explained by the fact that the four droplets are dispensed after each other and the extracted amount is increased if the droplets are connected earlier. In contrast to the separation funnel, where the different organic phases are manually separated and combined in the end, the analyte is distributed to all spots containing 1-octanol during the extraction on the DMA. This might be a drawback if the extracted compound will be used for further experiments, but results in nearly complete removal of the compound from the starting spot. Using four droplets of the organic solvent at one time point, another facet of the parallel extraction on the DMA was shown to improve the extraction efficiency while reducing the time compared to repeated mixing and separating.

To investigate the extraction efficiency of much lower concentrations, MALDI-MS was used to analyze the amounts of compounds directly on-chip before and after extraction. Due to its flat and accessible format, the DMA is compatible with this highly sensitive analytical method.[5] MALDI-MS on a Bruker rapiflex showed a mass resolving power of 10 000, and a step-size of 100 µm was used for spatial resolution. The sample was prepared by extracting a dilution series of 250 nL aqueous droplet containing Rhodamine B in a concentration from 20 nM to 4 µM with 75 nL 1-octanol. After evaporation of the aqueous droplets, 1-octanol was removed by evaporation under reduced pressure. Then, 50 nL 0.1 M alpha-hydroxycinnamic acid in water/acetonitrile (1:1) were dispensed into each spot (Figure S5A, Supporting Information). The whole slide was analyzed by MALDI-MS resulting in an ion image for m/z = 443.24 +/− 0.04 ($[M^+-Cl^-]$) (Figure 3C) as the main peak in the spectrum (Figure S5, Supporting Information)I. Starting from 50 fmol per spot, which equals a 250 nL water droplet with a concentration of 200 nM Rhodamine B, there is a clear signal detected on the 1-octanol spot, while the intensity for the initial aqueous spot is negligibly low (Figure 3D, right). Compared to a control region, where the same solutions were printed without being extracted (Figure 3D, left), the transfer of Rhodamine B in low concentrations could be shown. The extraction was calculated by comparing the mean intensity for the aqueous and organic spot and shows high values even at low concentrations (Figure 3E). Those results suggest effective extraction even at low concentrations, in combination with the possibility to completely remove the organic solvent after the extraction, which is demonstrated in Figure S2D, Supporting Information. This makes the method suitable for biological assays requiring low drug concentrations in the low µM to nM range.[27]

Next, we investigated the selective extraction of Rhodamine B from a mixture containing methylene blue to mimic more complex mixtures. Methylene blue shows a higher affinity to water than to 1-octanol and is therefore not extracted (**Figure 4**B). Figure 4A shows a part of one DMA slide containing 250 nL aqueous droplets with either 0.2 mM Rhodamine B (Figure 4A, top), 0.83 mM methylene blue (Figure 4A, center), or a mixture of both dyes in the respective concentration (Figure 4A, bottom). Six repetitions of each condition were prepared in parallel and merged with 100 nL 1-octanol in one dispensing step. After separation of the droplets, 100 nL water was dispensed again on the initial aqueous spot to redissolve the analytes for imaging. The color of the droplets was determined by the *a* value in the CIELAB color space, which differentiates between a pink color with high positive values and a blue color with negative values. In Figure 4C, the respective value for the initial aqueous droplet and both droplets after extraction are presented. The background represents the color for the respective *a* value. For the methylene blue solution, the intensity of blue color of the aqueous droplet was compared before and after the extraction and no significant differences were observed, while the organic droplet stayed colorless. For Rhodamine B, the transfer of the dye from the aqueous droplet to the 1-octanol droplet was observed as before. For separation, methylene blue and Rhodamine B were mixed and the intense violet solution was merged with the 1-octanol droplet. Methylene blue remained in the aqueous donor droplet while Rhodamine B was transferred to the organic acceptor droplet, which can be seen by an increase of the *a* value in the organic phase from 4.0 to 7.6 like the Rhodamine B control (8.4), while the aqueous droplet shows negative *a* value of −2.1 close to the methylene blue control (−3.0). For better visualization, one droplet is shown in Figure 4C exemplarily in higher magnification for each time point. The separation was also monitored via MALDI-MS (Figure S5D, Supporting Information).

In the separation funnel, the separation of the two phases after extraction is based on gravity. The solvent with a higher density is accumulating at the bottom of the funnel and can be easily collected. In Figure 4D, 1-octanol with a lower density (0.826 g mL^{-1})[33] than water (0.997 g mL^{-1})[33] accumulated on top, while 2-bromotoluene with a higher density (1.423 g mL^{-1})[33] is forming the lower layer (Figure 4D). The position of the organic phase depends solely on their respective density and can be therefore challenging when varying the solvent system in an automated process. In contrast, on the DMA the separation is horizontal. Figure 4E shows the extraction of

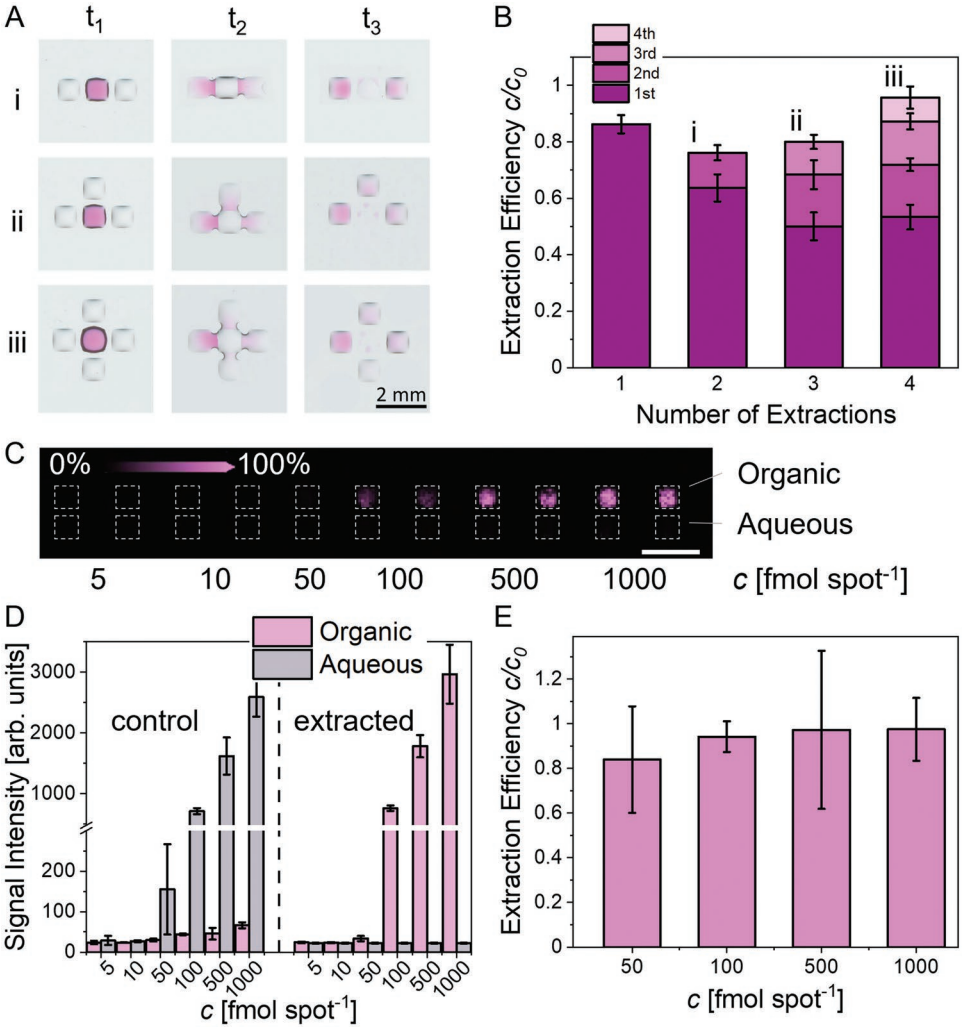

Figure 3. Optimization and scope of the on-chip extraction. A) Multiple extractions on one spot to increase the extraction efficiency. The spots are all merging at the same time to accelerate the time-consuming step. The droplets are shown for two, three, and four (i–iii) extractions before (left), during (middle) and after the merging (right). Scale bar is 2 mm. B) Extraction efficiency calculated based on the color intensity for single to four times extractions on one droplet. C) Ion intensity image for $m/z = 443.24 +/- 0.04$ from MALDI-MS measurement of an extracted dilution series of Rhodamine B ranging from 5 (left) to 1000 fmol per spot. Scale bar is 2 mm. D) Ion Intensity of MALDI-MS measurement for the aqueous (grey) and organic spot (pink) without (left) and after (right) extraction from different starting concentrations of Rhodamine B. The intensity values and error bars are calculated as mean from three different spots. E) The extraction efficiency of the extraction of different concentrations of Rhodamine B is calculated based on the MALDI-MS measurement. C_0 is calculated as sum of the final and initial spot. The mean values of three measurements were taken and the error bars result from Gaussian error propagation calculation.

0.2 mM Rhodamine B and 0.85 mM methylene blue aqueous solution. 250 nL of the aqueous droplet were dispensed on the left spot (Figure 4E, before). 1-octanol or 2-bromotoluene were then printed as 100 nL droplet on the right neighboring spot to merge with the aqueous droplet. The extraction could be observed for both solvents by the color change of the aqueous droplet on the left (Figure 4E, extract). For 2-bromotoluene, the loss of pink color of Rhodamine B is known for non-protic solvents.[34] After evaporation, 100 nL of water was dispensed to all spots to show that the extracted pink dye was transferred to the right spot for both solvents—independently of gravity, and thereby independent of the solvent system (Figure 4E, after).

Furthermore, 100 nL of toluene with a higher vapor pressure (3.79 kPa)[32] than water was used as organic phase in Figure 4F in combination with the yellow dye bromothymol blue to show the extraction from the organic droplet into a 250 nL water droplet. Toluene was evaporated after 30 s first, followed by the water droplet. In this case, the extraction still takes place, as the yellow dye is transferred to the aqueous droplet on the left. Figure 4E,F shows that the successful extraction is not depending on the density and vapor pressure of the used solvents. This facilitates the planning and automatization of experiments enormously. The extracting solvent can be changed between different repetitions or within one DMA slide without requiring a change of the dispensing plan in the whole process.

In the last part, we demonstrated an application of the method for the separation of two chemical compounds based on their *pKa* value. To show the selective transfer of the reagent

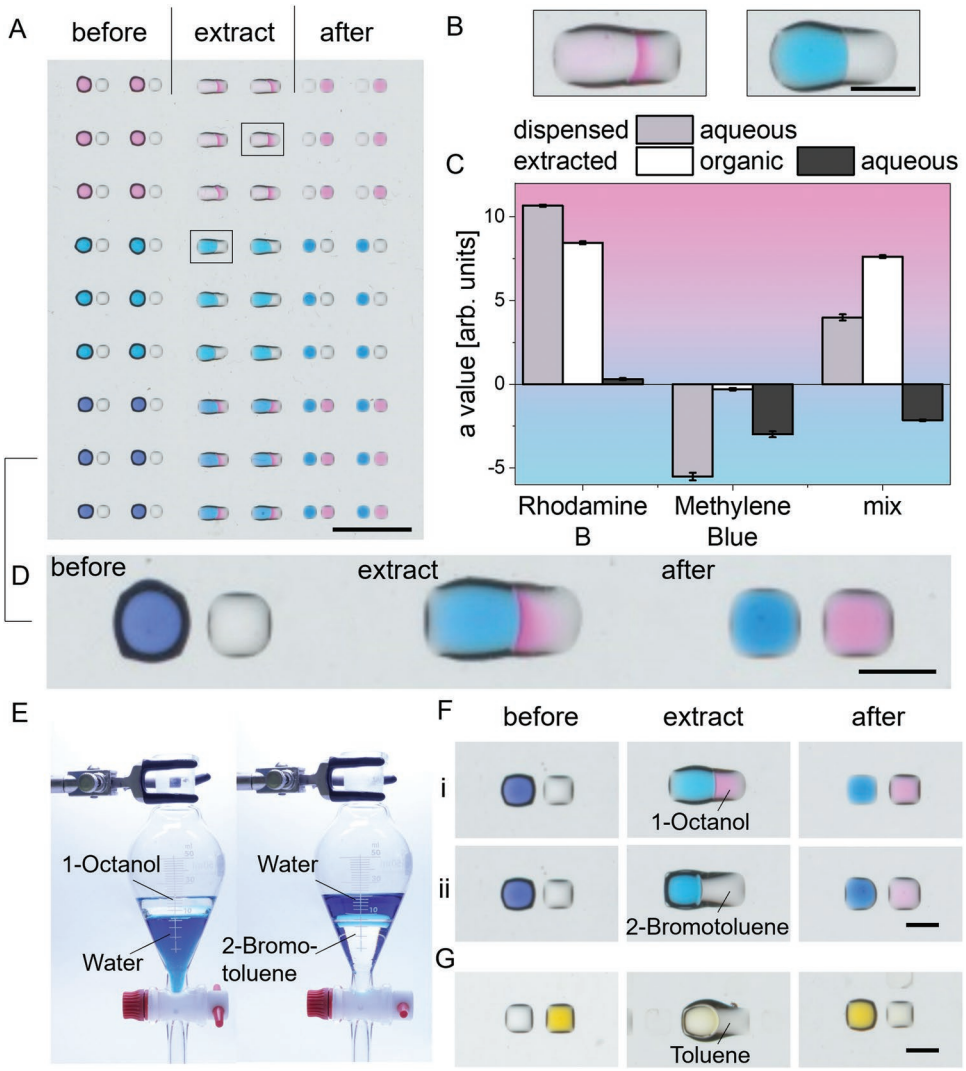

Figure 4. Separation of complex mixtures: A) scanned image of the extraction of an aqueous solution containing Rhodamine B only (top), methylene blue only (center), and a mixture of both dyes (bottom). 250 nL of the aqueous solutions are dispensed on the left spot with six repetitions, each (before), after addition of 100 nL 1-octanol to the right (extract) and after evaporation and subsequent addition of water to all spots (after). Scale bar is 5 mm. B) For Rhodamine B (left) and methylene blue (right), one extracting droplet is shown in higher magnification with a scale bar of 1 mm. C) Mean a value for single spots from the scanned image of a lab stack file for the starting solutions (grey), the extracted organic droplet (white), and the remaining aqueous droplet (black) for the single and mixed dyes. D) Scanned image of the separation of the mixture of dyes for one droplet before, during, and after extraction with a refilled water droplet. Scale bar is 1 mm. E) Phase separation in the separation funnel with 18 mL water (blue) and 18 mL 1-octanol (left) or 2-bromotoluene (right). F) Extraction of a mixture of Rhodamine B and methylene blue with 1-octanol (i) and 2-bromotoluene (ii) on the right neighbored spot. Scale bar is 1 mm. G) Extraction of 2-bromothymol blue from toluene (right) to the aqueous droplet (left). Scale bar is 1 mm.

of interest to the neighbored spot, a carboxylic acid, 2,5-dihydroxybenzoic acid (DHB), and an aromatic amine, *p*-anisidine, were extracted. Both reagents show a positive log *P* value (DHB 1.74,[35] *p*-anisidine 0.95[36]) and are therefore extracted to 1-octanol in their non-charged state, but the respective salts are retained in the aqueous phase (**Figure 5**A). Thin layer chromatography (TLC) was used to detect the compounds in the organic phase (Figure S5, Supporting Information) by collecting them with a capillary directly from the DMA slide (Figure S6A, Supporting Information). With the solvent mixture of dichloromethane/methanol/acetic acid (89/10/1), the compounds could be identified by the R_f value of 0.33 for DHB and 0.83 with a second spot at $R_f = 0.55$ for *p*-anisidine, containing some *o*-anisidine (Figure 5B and Figure S6B,C, Supporting Information). The TLC shows for the organic phase extracted from the basic solution only the spots for the amine, while the sample extracted from the acidic solution shows the spot for the acid only (Figure 5B). In the next step, the pH value of the aqueous solution was changed after the first extraction step from basic to acidic by refilling the evaporated aqueous spot with 0.1 M HCl solution. Subsequently, the solution was extracted again with 1-octanol, but to the neighboring droplet on the opposite site. Also in this case, the TLC showed the signal for the amine after the first extraction and the acid only for the second extraction. This result shows that a sample solution can be manipulated in a way that the compound of interest can selectively be

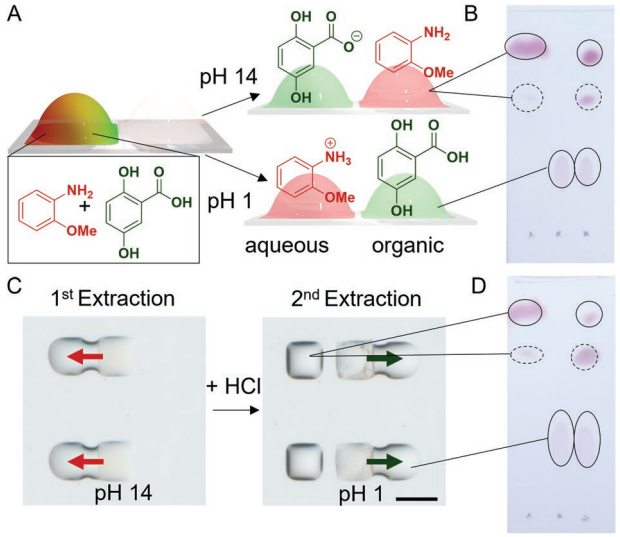

Figure 5. pH-dependent separation: A) scheme for the selective separation of an organic acid (2,5-dihydroxybenzoic acid) and amine (*p*-anisidine) on the DMA based on the pH value. B) TLC images for the organic droplets after the extraction at pH 14 (left) at pH 1 (center). As control, the mixture of both reagents was added on the right. The R_f values for the amine are 0.83 and 0.55, and for DHB 0.33. The TLC was developed in dichloromethane with 10% methanol and 1% acetic acid, and stained with iodine vapor. C) Sequential separation of a mixture of DHB and *p*-anisidine. After the first extraction with 75 nL 1-octanol on the left, the evaporated aqueous spot is filled with 200 nL 1 M HCl and the second extraction step to the right neighboring droplet is initiated. Scale bar is 1 mm. D) Image of the TLC of the first 1-octanol droplet (left), the second 1-octanol droplet (center), and the mixture of both compounds (right).

isolated on the neighbored spot. With that method, it becomes possible to perform the reaction workup after synthesis to remove biologically active side reagents or toxic catalysts. This enables analysis of a synthesized compound on the same platform without any manual transferring steps.

3. Conclusion

In summary, we presented a new method for highly miniaturized and parallelized separation of mixtures of compounds using the droplet microarray platform. The method is based on the possibility to merge neighboring nanoliter droplets without losing special arrangement, which was demonstrated by performing 192 parallel extractions using only 52 µL of liquid in total. Furthermore, several more complex techniques were successfully transferred from bulk handling to our system, as the repeated extractions of one aqueous solution or the change of pH for more sophisticated separations. Compared to the separation funnel, the solutions do not need to be manually transferred, for example to a microtiter plate for biological tests. This can save time, avoid manual handling steps and, therefore, reduce loss of compounds, but also rules out the possibility of combining several extracted phases or further dilution steps. The fast extraction time of few minutes was sufficient to achieve an extraction efficiency of up to 90% in the experiments with Rhodamine B, maintaining a high efficiency by decreasing the handled amount of analyte to femtomoles. It was also shown that the extraction efficiency could be improved by varying parameters such as the humidity for a prolonged extraction time or the ratio of solvents used. The whole process consists of two dispensing steps, which can be easily automatized and do not require any additional handling like agitation or sonication. The small format and, thus, fast evaporation limit the choice of organic solvents to those with high boiling points like 1-octanol, compared to commonly used solvents like dichloromethane or hexane. Still, there is a new range of solvents that can be discovered, also in regard of lower toxicity. Furthermore, even high boiling point solvents like 1-octanol could be completely removed by evaporation under reduced pressure within 1 h, so that the choice of solvents does not affect following steps like a biological screening or analytics. The gravity independent separation facilitates planning and automatization steps, as solvents with different densities can be used in one step without adapting the further handling. Furthermore, the addition of acids or bases between the extraction steps allows the selective separation of single compounds from a complex solution of reagents. The open, flat array format allows the fast optical readout by a document scanner. In addition, MALDI-MS was used to determine the extraction efficiency, by performing the measurement directly on the DMA platform. All of this shows the potential of the nanoliter sized extraction to be included in the drug development pipeline from the chemical synthesis, including the purification, to the final biological screening or characterization with MALDI-MS. We believe that this method is a powerful tool and a missing link in the chemBIOS workflow for miniaturized high-throughput synthesis, purification, and biological screening united on one versatile platform to increase the efficiency in early-stage drug discovery.

4. Experimental Section

Materials and Chemicals: NEXTERION Glass B microscopic glass slides were bought from SCHOTT Technical Glass Solutions GmbH (Jena, Germany)

Acetone, ethanol, and 2-propanol at technical grade were purchased from MERCK KGaA (Darmstadt, Germany). For MALDI-MS measurements, UHPLC grade acetonitrile and water from Sigma-Aldrich (Darmstadt, Germany) were used.

Triethoxyvinylsilane, 2,2-dimethoxy-2-phenylacetophenone (DMPAP), 4-pentenoic acid, 1-thioglycerol, Rhodamine B, 1H,1H,2H,2H-perfluorodecanethiol (PFDT), *p*-anisidine, 2,5-dihydroxybenzoic acid, alpha-hydroxycinnamic acid and 1-octanol were purchased from Sigma-Aldrich (Darmstadt, Germany). *N,N′*-Diisopropylcarbodiimide (DIC) was purchased from Alfa Aesar–Thermo Fisher GmbH (Kandel, Germany). Bromothymol blue was purchased from VWR International GmbH (Darmstadt, Germany). 4-(dimethylamino)pyridine (4-DMAP) was bought from Novabiochem (Darmstadt, Germany). Methylene blue hydrate was purchased from Fluka. All chemicals were used without further purification.

Photomasks were bought from Rose Fotomasken (Bergisch Gladbach, Germany)

UV Cuvettes were bought from BRAND GmbH and Co. KG (Wertheim, Germany)

Capillary tubes were purchased from Marienfeld (Lauda Königshofen, Germany)

ALUGRAM Xtra SIL G/UV$_{254}$ plates for TLC were purchased from Machery–Nagel (Düren, Germany)

Preparation of Dendrimer DMA Slides: The Dendrimer slides were prepared according to the procedure described by Benz et al.[5] The procedure is described shortly below. The microscopic glass slides were activated by UV treatment with an UVO-cleaner 42–220 from Jelight Company Inc. (California, USA) and silanized with triethoxyvinylsilane in gas phase for 16 h at 80 °C. Three dendrimer generations were created by repeating an UV activated tiol-ene click reaction and an esterification step. For the thiol-ene reaction, a solution of 10% v/v thioglycerol and 1 wt% DMPAP in ethanol/water (1:1) was added to the glass surface and irradiated for 2 min at 260 nm UV light. For esterification, the slide was placed in 50 mL of acetone containing 4-DMAP (56 mg, 458 µmol), 4-pentenoic acid (125 µL, 127 mg, 1.27 mmol), and 180 µL DIC (180 µL, 220 mg, 1.75 mmol) for 4 h. In the last modification step, a 10% v/v solution of 1H,1H,2H,2H-perfluorodecanethiol in isopropanol was used with a photomask that covered the omniphilic spots, before the thioglycerol solution was used. The slides were modified in the photolithographic step with a photomask that creates 1152 omniphilic square spots on one slide. The spots have a dimension of 900 × 900 µm and are separated by an omniphobic border of 125 µm.

Extraction in Bulk: For extraction in a separation funnel, of 0.2 mM aqueous solution of Rhodamine B was added first, followed by 1-octanol. The extraction was carried out for 1 min either under constant shaking or without any moving. The phases were separated, and 1 mL of each phase was taken for spectrophotometric quantification

Dispensing of Droplets: For all dispensing steps, CERTUS FLEX from Fritz Gyger AG (Gwatt, Switzerland) was used. The aqueous solution was dispensed with either 0.1 or 0.3 bar. 1-octanol was printed with 0.6 bar, for 2-bromotoluene, toluene, and cyclohexanone, a pressure of 0.3 bar was used. For the extraction process, 100–300 nL of an aqueous solution was printed first. The organic solvents were dispensed with a printing scheme that was shifted by −875 µm with a volume of 75–100 nL. The slide was placed in an opened hood until the separation of the droplets was completed.

For the extraction of *p*-anisidine and DHB, 200 nL of a solution containing 0.5 M of each compound was dispensed. The pH value was either adjusted before with 1 M hydrochloric acid or 1 M sodium hydroxide solution, or on the slide by addition of 210 nL of 0.1 M hydrochloric acid. 75 nL 1-octanol were added to each spot to initiate the extraction.

Image Acquisition and Analysis: Brightfield videos were taken with the microscope Keyence BZ9000 from Keyence Deutschland (Neu-Isenburg, Germany). The images were recorded with an ×4 objective (Nikon ×4 Plan Apo NA 0.20/20 mm) with a resolution of 8-bit. The exposure time was adjusted to avoid saturation of pixels.

Images of the Droplet Microarray were taken with the scanner CanoScan 8800F from Canon Deutschland GmbH (Krefeld, Germany) at 70% exposure at different time points during the extraction procedure. The images are shown in the figures without any color modification. The RGB images were converted into HSV stack with ImageJ. 25 spots were picked randomly and the saturation intensity was measured of a square of 256 × 256 pixels. The median was calculated from the replicates with standard deviation. To calculate the actual concentration, a dilution series of Rhodamine B in 1-octanol was measured and analyzed as described above. For methylene blue/Rhodamine B separation, the mean *a* values for 256 × 256 pixels of the Lab stack image were measured and the value for the empty spot was subtracted. The standard deviation was calculated out of three repetitions.

UV/Vis: UV/vis spectra were measured with a blank of 1 mL deionized water with autocorrection. Absorbance spectra of aqueous solutions with different concentrations of Rhodamine B (0.2, 0.4, 0.8, 1, 2, 4, 8, and 20 µM) were measured at 300–700 nm in cuvettes with a thickness of 1 cm with a Lambda 35 UV/Vis Spectrophotometer from PerkinElmer (Massachusetts, USA). With Lambert–Beer's Law, an extinction coefficient ε (554 nm) = 87 793 ± 482 M^{-1} cm^{-1} was calculated.

MALDI-MS: Extraction of different concentrations of Rhodamine B aqueous solutions with 1-octanol were conducted as described before. After removing the solvents under reduced pressure over night, 50 nL of 0.1 M alpha-hydroxycinnamic acid in water/acetonitrile (1:1) was dispensed on each spot and dried in the hood. Before starting the measurement, the back side of the sample was covered with a conductive tape (Figure S5, Supporting Information).[37]

MALDI-TOF MSI measurements were performed on a rapifleX MALDI Tissuetyper (Bruker Daltonics GmbH, Bremen) in reflector positive operation mode with a raster size of 100 µm. For each data point, ion intensities emerging from 200 laser shots were accumulated at a repetition rate of 10 000 Hz. The laser fluency was set to 25%. Spectra were recorded in a mass range from 100 to 600 Da. Calibration of the mass spectra was done by clusters of red phosphorus[38] in cubic enhanced mode.

Data analysis was initially performed in SCiLS Lab MVS (Bruker Daltonics GmbH, Version 2022b Pro). Mass features were selected, and the corresponding ion images were exported as imzML format using the reduced feature list, total ion count normalization and peak area. Exported ion images were analyzed in a Python3.8 script using the pyimzml parser (Fay D. pyimzML parser for the imzML format. https://github.com/alexandrovteam/pyimzML) for data import. For each DMA spot, the sum intensity for a given spot was calculated and used for further analysis. For final plotting, calibration of the m/z value was done using the matrix peak at m/z = 190.049.

TLC: For TLC, plates with silica gel coated with fluorescent indicator F254 from MERCK were used. The compounds were added with a capillary on the plate and placed in a TLC chamber with the respective solvent. For separation of *p*-anisidine and DHB, dichloromethane/methanol/acetic acid (89:10:1) was used as solvent. The compounds were stained with iodine vapor and the plates were imaged with a digital camera.

Water Contact Angle: The static angle of droplets of water and 1-octanol on the omniphilic and omniphobic surface were measured with a Drop Shape Analyzer DSA25 from Krüss GmbH (Hamburg, Germany) and evaluated with the software Krüss Advance 1.6.2.0.

Supporting Information

Supporting Information is available from the Wiley Online Library or from the author.

Acknowledgements

J.J.W. and Y.N.D. contributed equally to this work. This project was partly supported by the DFG (Heisenbergprofessur Projektnummer: 406 232 485, LE 2936/9-1) and by the BMBF project "Drugs4Future" within the M2Aind consortium (13FH8I05IA). Furthermore, the authors thank the Impuls- und Vernetzungsfond (IVF) of the Helmholtz Association. This research was supported by the Ministry of Science, Research, and the Arts of Baden–Württemberg within a funding program "Ideas competition biotechnology—learning from nature" (7533-7-11.10-12). Y.W. thanks funding of the research through the Gottfried–Wilhelm Leibniz prize NE 822/31-1 of the German research foundation (DFG). F.W. is grateful to the VirtMat project P09 "Wetting Phenomena" of the Helmholtz association (MSE program no. 43.31.02). The authors acknowledge support by the state of Baden–Wuerttemberg through bwHPC. M.K. thanks the Carl Zeiss Foundation for financial support. The authors thank J. L. Cairns and J. Huber for their contribution in MALDI MS data acquisition and N. Holz and J. Biesinger for performing extraction experiments. The authors also thank Pragya Parihar for literature research about miniaturized extraction techniques. Figure 1 was created with BioRender.com.

Open access funding enabled and organized by Projekt DEAL.

Conflict of Interest

The authors declare no conflict of interest.

Data Availability Statement

The data that support the findings of this study are available from the corresponding author upon reasonable request.

Keywords

droplet microarray, high-throughput, liquid–liquid extraction, miniaturization, parallelization, reaction workup, separation

Received: July 21, 2022
Revised: October 28, 2022
Published online:

[1] P. Bhutani, G. Joshi, N. Raja, N. Bachhav, P. K. Rajanna, H. Bhutani, A. T. Paul, R. Kumar, *J. Med. Chem.* **2021**, *64*, 2339.
[2] a) G. A. Van Norman, *JACC: Basic Transl. Sci.* **2016**, *1*, 170; b) H. C. S. Chan, H. Shan, T. Dahoun, H. Vogel, S. Yuan, *Trends Pharmacol. Sci.* **2019**, *40*, 592.
[3] B. S. Alexander, E. Regalado, T. Pereira, M. Shevlin, K. Bateman, L.-C. Campeau, J. Schneeweis, S. Berritt, Z.-C. Shi, P. Nantermet, *Science* **2015**, *347*, 49.
[4] M. Benz, M. R. Molla, A. Böser, A. Rosenfeld, P. A. Levkin, *Nat. Commun.* **2019**, *10*, 2879.
[5] M. Benz, A. Asperger, M. Hamester, A. Welle, S. Heissler, P. A. Levkin, *Nat. Commun.* **2020**, *11*, 5391.
[6] M. Brehm, S. Heissler, S. Afonin, P. A. Levkin, *Small* **2020**, *16*, 1905971.
[7] G. Schneider, *Nat. Rev. Drug Discovery* **2018**, *17*, 97.
[8] D. J. Payne, M. N. Gwynn, D. J. Holmes, D. L. Pompliano, *Nat. Rev. Drug Discovery* **2007**, *6*, 29.
[9] R. J. Booth, J. C. Hodges, *J. Am. Chem. Soc.* **1997**, *119*, 4882.
[10] a) N. Cankařová, V. Krchňák, *Int. J. Mol. Sci.* **2020**, *21*, 9160; b) P. Andrade-Gordon, B. E. Maryanoff, C. K. Derian, H. C. Zhang, M. F. Addo, A. L. Darrow, A. J. Eckardt, W. J. Hoekstra, D. F. McComsey, D. Oksenberg, E. E. Reynolds, R. J. Santulli, R. M. Scarborough, C. E. Smith, K. B. White, *Proc. Natl. Acad. Sci. USA* **1999**, *96*, 12257.
[11] T. M. Doran, P. Dickson, J. M. Ndungu, P. Ge, I. Suponitsky-Kroyter, H. An, T. Kodadek, in *Methods in Enzymology*, (Ed: A. K. Shukla), Academic Press, Cambridge, MA **2019**, pp. 91–127.
[12] G. Schnorrenberg, H. Gerhardt, *Tetrahedron* **1989**, *45*, 7759.
[13] R. Frank, *Tetrahedron* **1992**, *48*, 9217.
[14] a) R. Frank, *J. Immunol. Methods* **2002**, *267*, 13; b) Q. Lin, J. C. O'Neil, H. E. Blackwell, *Org. Lett.* **2005**, *7*, 4455.
[15] S. P. A. Fodor, L. J. Read, M. C. Pirrung, L. Stryer, A. T. Lu, D. Solas, *Science* **1991**, *251*, 767.
[16] A. Rosenfeld, M. Brehm, A. Welle, V. Trouillet, S. Heissler, M. Benz, P. A. Levkin, *Mater. Today Bio* **2019**, *3*, 100022.
[17] H. C. Kolb, M. G. Finn, K. B. Sharpless, *Angew. Chem., Int. Ed.* **2001**, *40*, 2004.
[18] C. L. Barhate, A. F. Donnell, M. Davies, L. Li, Y. Zhang, F. Yang, R. Black, G. Zipp, Y. Zhang, C. L. Cavallaro, E. S. Priestley, H. N. Weller, *Chem. Commun.* **2021**, *57*, 11037.
[19] F. Sutanto, S. Shaabani, R. Oerlemans, D. Eris, P. Patil, M. Hadian, M. Wang, M. E. Sharpe, M. R. Groves, A. Dömling, *Angew. Chem., Int. Ed.* **2021**, *60*, 18231.
[20] Y. Shen, B. Chen, H. Zuilhof, T. A. van Beek, *Molecules* **2021**, *26*, 38.
[21] B. Mahjour, Y. Shen, T. Cernak, *Acc. Chem. Res.* **2021**, *54*, 2337.
[22] A. Sarafraz-Yazdi, A. Amiri, *TrAC, Trends Anal. Chem.* **2010**, *29*, 1.
[23] S. X. Peng, C. Henson, M. J. Strojnowski, A. Golebiowski, S. R. Klopfenstein, *Anal. Chem.* **2000**, *72*, 261.
[24] W.-H. Sun, Y. Wei, X.-L. Guo, Q. Wu, X. Di, Q. Fang, *Anal. Chem.* **2020**, *92*, 8759.
[25] S. S. Wells, R. T. Kennedy, *Anal. Chem.* **2020**, *92*, 3189.
[26] a) W. Feng, L. Li, E. Ueda, J. Li, S. Heißler, A. Welle, O. Trapp, P. A. Levkin, *Adv. Mater. Interfaces* **2014**, *1*, 1400269; b) A. A. Popova, K. Demir, T. G. Hartanto, E. Schmitt, P. A. Levkin, *RSC Adv.* **2016**, *6*, 38263.
[27] A. A. Popova, S. Dietrich, W. Huber, M. Reischl, R. Peravali, P. A. Levkin, *SLAS Technol.* **2020**, *26*, 274.
[28] C. RamalloGuevara, D. Paulssen, A. A. Popova, C. Hopf, P. A. Levkin, *Adv. Biol.* **2021**, *5*, 2000279.
[29] a) H. Cui, X. Wang, J. Wesslowski, T. Tronser, J. Rosenbauer, A. Schug, G. Davidson, A. A. Popova, P. A. Levkin, *Adv. Mater.* **2021**, *33*, 2006434; b) G. E. Jogia, T. Tronser, A. A. Popova, P. A. Levkin, *Microarrays* **2016**, *5*, 28; c) W. Lei, K. Demir, J. Overhage, M. Grunze, T. Schwartz, P. A. Levkin, *Adv. Biosyst.* **2020**, *4*, 2000073.
[30] Y. Wu, M. Kuzina, F. Wang, M. Reischl, M. Selzer, B. Nestler, P. A. Levkin, *J. Colloid Interface Sci.* **2022**, *606*, 1077.
[31] Comptox Chemicals Dashboard, https://comptox.epa.gov/dashboard/chemical/details/DTXSID6042369 (accessed: June 2022).
[32] T. E. Daubert, R. P. Danner, *Physical and Thermodynamic Properties of Pure Chemicals: Data Compilation*, Taylor and Francis, Washington DC **1989**.
[33] W. M. Haynes, D. R. Lide, *CRC Handbook of Chemistry and Physics*, 95th ed., CRC Press, Boca Raton, FL **2014**.
[34] H. N. Kim, M. H. Lee, H. J. Kim, J. S. Kim, J. Yoon, *Chem. Soc. Rev.* **2008**, *37*, 1465.
[35] Y. He, H. K. Lee, *Anal. Chem.* **1997**, *69*, 4634.
[36] C. Hansch, A. Leo, D. Hoekman, *Exploring QSAR.: Hydrophobic, Electronic, and Steric Constants*, American Chemical Society, Washington, DC **1995**.
[37] M. J. Weissenborn, J. W. Wehner, C. J. Gray, R. Šardzík, C. E. Eyers, T. K. Lindhorst, S. L. Flitsch, *Beilstein J. Org. Chem.* **2012**, *8*, 753.
[38] K. Sládková, J. Houska, J. Havel, *Rapid Commun. Mass Spectrom.* **2009**, *23*, 3114.